IIETA International Information and Engineering Technology Association
Advancing the World of Information and Engineering

Annales de Chimie - Science des Matériaux
Vol. 44, No. 5, October, 2020, pp. 311-318
Journal homepage: http://iieta.org/journals/acsm

Preparation and Characterization of Matrix Hybrid Membranes Polyvinylidene Fluoride/Polyvinylpyrrolidone/Silica Gel/Zinc Oxide for Cr(VI) Removal from Water

Mustapha Chabane[1,2*], Chikh Melkaoui[3], Benamar Dahmani[1], Sihem Zahia Belalia[1]

[1] Laboratory of Research on Spectrochemistry and Structural Pharmacology, Department of Chemistry, Science Faculty, University of Tlemcen, Tlemcen 13000, Algeria
[2] Department of Technology, Institute of Science and Technology, University Center of Naama, Ctr Univ Naama, Box 66, Naama 45000, Algeria
[3] Center for Scientific and Technical Research in Physical and Chemical Analysis (CRAPC), PO Box 384 Bousmail Tipaza 42004, Algeria

Corresponding Author Email: chabane@cuniv-naama.dz

https://doi.org/10.18280/acsm.440502

Received: 24 December 2019
Accepted: 16 September 2020

Keywords:
chromium, hybrid, membrane, PVDF, silica gel, ZnO

ABSTRACT

Matrix hybrid membranes, based on polyvinylidene fluoride (PVDF), poly (N-vinylpyrrolidone) (PVP), silica gel (SG) and zinc oxide (ZnO) were synthesized by phase inversion via immersion precipitation method. The characterization of membrane samples was performed using Fourier transform infrared spectroscopy (FTIR), X-ray diffraction (XRD), optical microscopy, contact angle, porosity, mean pore size and water permeability measurements. The FTIR analysis showed the appearance of new bands attributed to the functional groups of SG and ZnO. The XRD analysis confirmed a modification in the structure of membranes. The prepared membranes were used for the removal of hexavalent chromium (Cr(VI)) from aqueous solution. Membrane filtration experiments show that the water permeability and Cr(VI) rejection ratios increase with increasing the weight ratio ZnO (%)/SG (%). The maximum values of the Cr(VI) rejection rate and water permeability were respectively 85% and 685 L/m^{2}hbar for weight ratios (0.75% of ZnO/0.25% of SG).

1. INTRODUCTION

Hexavalent chromium [Cr(VI)] is considered as toxic substance with a dangerous effect for human health, causing serious diseases due to a change in DNA structure leading to the tumors growth [1]. The pollution of water sources by Cr(VI) is mainly caused by different industrial discharges from the tanning of leather, electroplating ,the manufacture of chemical products and metals alloys [2]. In this regards, different methods have been applied for the removal of Cr(VI) from water, such as photocatalysis, mineral muds, granulated carbon, filtration, electrochemical method and ultrasonic cavitation [3, 4]. In general, these techniques were found to be disadvantageous; this is due to several factors such as the high energy consumption, fouling phenomenon; damage effect for the environment by using of the chemical products inlet the processes and also the saturation phenomenon of the adsorbents, which require regeneration or renewed of the adsorbent supports and therefore an increase the water treatment cost [4, 5]. Table 1 summarizes the advantages and disadvantages of different methods used for Cr(VI) removal from water .

Indeed, the use of some materials and technologies for Cr(VI) present some problems in industrial applications. Specially in waste water treatment plants.

In recent years; the separation of solute species using low pressure porous membranes such ultrafiltration are considered as a promised alternative for water treatment, because this technology requires low energy consumption, operational simplicity and no chemical products used [6]. However, some ultrafiltration membranes have limitations with respect to selectivity of toxic dissolved species, fouling phenomenon by macromolecules and low water permeability due to the hydrophobic character In fact The membrane surface coating by some polymers such as N-vinyl-2-pyrrolidinone (NVP), polymethacrylic acid (PMAA) and Poly(ethylene glycol) (PEG) increase the contact angles and decrease the pure water flux and consequently promotes accumulation of solutes on the pore surface [7]. In order to overcome these problems, the modification of original membranes structures by incorporating of different inorganic and organic materials into the polymeric matrix was approved as reliable methods for improving more the water permeability and solute separation efficiency from water supplies.

PVDF is considered to be a leading polymer on the manufacturing of membranes, this is due to the mechanical resistance, chemical stability, flexibility and thermal resistance [7]. Moreover, these properties allow to use PVDF for the preparation of the ultrafiltration membranes by mixed PVDF with different additives for enhancement the pores sizes and separation of molecules. The functional structures of the additives are considered to be an important element for the pore formation, such as poly(N-vinylpyrrolidone) (PVP) and/or retention of molecules in the surface of the membranes. it was reported from the literature that synthetic ultrafiltration membranes based on PVDF and 2aminobenzothiazole reject 82% of Cr(VI) from waste water, this result is mainly due to the excellent adsorption properties of the Cr(VI) ions by

2aminobenzothiazole,this is due to the clathrate effect of functional groups =C–H and H–C–H with chromium ions [8].

However, the synthetic organic additives present some limitations related to the high cost, low mechanical and chemical resistance; and also, their harmful effect to the environment. For this purpose, natural inorganic additives such as titanium dioxide (TiO_2), zirconium dioxide (ZrO_2), Silica (SiO_2), Alumina (Al_2O_3), Zinc Oxide (ZnO) [9] may represent a real alternative on the improvement of the performance and characteristic of matrix hybrid PVDF membrane .Among the inorganic materials cited, silica gel (SG) and ZnO are considered as excellent nanoparticles with high adsorption capacity of Cr(VI) ions. This is due to the geometry of the pores, the specific surface, their high porosity, great mechanical and thermal resistance [10]. It was reported that composite nanofiber PAN/GO synthesized by electrospinning techniques and decorated with ZnO adsorb Cr(VI) ions above 690 mg/g [10]; Gang et al. [11] have prepared new adsorbents for removing Cr(VI) by incorporating SG to polymer structures during the polymerization mechanism, it was found that the rejection efficiency of Cr(VI) ions by modified PVP coated SG reached 100% at initial concentration of 2.5 mg/L and pH=5 In other experiment, Karthik et al. [12] used SG nanoparticles as additive during polymerization of (PANI/SiO_2);the results showed that the synthesized materials can adsorb Cr(VI) ions above 63.3 mg/g at 303K, According to the referenced studies, it will be interessant to study the combined effect of SG and ZnO used as inorganic additives in the preparation of matrix hybrid membranes and their application on the remove of Cr(VI) from water. The aim of this research work is to prepare matrix hybrid membranes based on polyvinylidene fluoride (PVDF), poly(N-vinylpyrrolidone) (PVP), silica gel (SG) and zinc oxide (ZnO) by the phase inversion method. The membrane samples were characterized by different techniques: Fourier transform infrared spectroscopy (FTIR), X-ray diffraction (XRD); optical microscopy, contact angle, porosity, mean pore size and water permeability. The rejection of Cr(VI) by the synthesized membrane samples was tested using dead end pilot unit.

The effect of the use of ZnO and SG as additives on the structural modification of hybrid matrix membranes was studied by the FTIR. XRD by comparison between the different spectra and patterns of the membrane samples .These inorganic additives on the evolution of the porosity, the pore sizes; hydrophilic or hydrophobic characters of the surface of membranes were studied by using experimental methods such as optical microscopy, membrane dry test, contact angle and calculation method .For the pure water permeability of each membranes were measured by the variation of the permeate flux of each versus transmembrane pressure using dead end pilot unit .The rejection of Cr(VI) by both membranes was studied in the same unit pilot and the rejection rate was calculated by determination of Cr(VI) concentration in feed and permeate samples.

2. MATERIAL AND METHODS

2.1 Reagents

In order to synthesize the hybrid matrix membranes and to study of Cr(VI) by both membranes , several reagents were used. The Table 2 summarizes the characteristics of each chemical products used in experimental test.

2.2 Preparation of standard solution

Standard solution with concentration of 100 ppm of chromium (VI) was prepared by successive dilution of stock solution of chromium (VI) stock solution with concentration of 1000 ppm. The method of preparation of stock solution consist on dissolution of 2.829 g of $K_2Cr_2O_7$ in 1 L of distilled water. The pH of the standard solution is 6.5 equivalent to the predominant species of CrO_4^{2-} species whose oxidation degree of chromium is +6. referring to different researches established [1-3].

2.3 Membranes synthesis method

As it was show in Table 3, homogeneous solutions were prepared by dissolving different amounts of PVDF, PVP, SG and ZnO in DMF. The Solutions were stirred for 8 h at temperature of 50°C, poured and casted on glass plate using casting knife. The immersion precipitation method the membranes was immersed into water. In order to ensure complete phase separation, the membranes were immersed in water for 1 day. Then, the membranes were immersed in ethanol for 1 day and n hexane for 3 h in order to ensure that all solvents are completely removed. At the final stage, the membranes were dried for 24 h.

Table 1. Advantages and disadvantages of Cr(VI) removal techniques [1]

Techniques	Advantages	Disadvantages
Adsorption by activated carbon	High adsorption capacity	High cost
Adsorption by Chitosan	Low cost	Requires chemical modification
Adsorption by inorganic membrane	High stability	High cost
Filtration by polymeric membrane	Less space requirement	Low stability; membrane fouling
Separation by liquid membrane	Low energy demand	Emulsion swelling in ELM
Filtration by membrane electrolysis	low maintenance	High cost
Electrochemical method	low cost	Production of sludge

Table 2. Technical and commercial data of chemical products

Reagents	Commercial name	Suppliers
Poly(vinylidene fluoride)	PVDF(UdelP1700)	Sigma Aldrich
Polyvinylpyrrolidone	PVP (K29-32)	Sigma Aldrich
Dimethylformamide	Dimethylformamide (ACS reagent, 99.7%)	Sigma Aldrich
Silica gel	Silica gel (99.9%)	Sigma Aldrich
$K_2Cr_2O_7$	Potassium dichromate, 99+%, ACS reagent	Fischer scientific
Zinc Oxide	Zinc oxide, puriss. p.a., ACS reagent, ≥99.0% (KT),	Merck

Table 3. Composition of casting solutions

Membranes	PVDF (%)	PVP (%)	SG (%)	ZnO(%)	DMF (%)
M1	18	2	0	0	80
M2	18	2	1	0	79
M3	18	2	0.75	0.25	79
M4	18	2	0.5	0.5	79
M5	18	2	0.25	0.75	79

2.4 Characterization of membranes

2.4.1 Fourier transformed infrared spectroscopy (FTIR) of the membrane samples

The membrane samples were completely dried at 50°C. before analysis and prepared in the form of KBr pellets. The FTIR analysis was carried out using a spectrophotometer (Spectrum, Perkin Elmer, USA), KBr pellets were placed on the sample holder and all the spectra were recorded in the range of wave numbers from 4000 to 400 cm^{-1} [13]

2.4.2 X-ray diffraction (XRD) study

The XRD diffraction patterns of the different types of membranes were analysed using made AXS Bruker D8 type powder diffractometer using Cu Kα radiation (λ= 0.154 nm). the range of the diffraction angles (2θ) from 5° to 90° under a constant voltage of 40 kV with tube current of 30 mA [13].

2.4.3 Optical microscopy

The surface of the membranes was carried by an ocular optical microscope with resolution 40X, this method of membranes observation has been used previously by Hu et al. [14].

2.4.4 Porosity and mean pore size

Membrane porosity is the defined as the ratio between pore volumes by the total volume of the porous membrane, as shown in the following equation [14].

$$\varepsilon = \frac{\frac{(\omega_{wet} - \omega_{dry})}{\rho_w}}{\frac{(\omega_{wet} - \omega_{dry})}{\rho_w} + \frac{\omega_{dry}}{\rho_w}} * 100 \quad (1)$$

The mean pore size was calculated according to Guerout Elford Fery equation [15, 16]:

$$r_m = \sqrt{\frac{(2.9 - 1.75 \times \varepsilon) \times (8 \times \eta \times \varepsilon \times Q_w)}{\varepsilon \times A_m \times \Delta P}} \quad (2)$$

2.4.5 Contact angle measurement

The hydrophilic property of synthesized matrix membranes was determined by the measurement of the contact angle between drop of distilled water and surface of the membrane. The instrument used for these experiments is DSA model supplied by KRUSS company [15].

2.4.6 Pure water permeability and rejection ratio of Cr(VI)

The water permeability L_p was measured for each synthesized membrane using dead end pilot unit (Amicon 8200) with an effective surface cell area of 29 cm^2, the filtration cell system was equipped with a nitrogen cylinder and gauge for pressure adjustment, the volume of permeate was measured using graduate funnel and the pure water permeability of membranes was calculated by the following equation:

$$L_P = \frac{V}{A_m \times t \times TMP} \quad (3)$$

The rejection ratio of Cr(VI) by synthetized membranes was studied using dead end pilot unit. The rejection rate of Cr(VI) was calculated using the following equation:

$$R(\%) = (1 - \frac{C_{permeate}^{Cr(VI)}}{C_{Feed}^{Cr(VI)}}) \times 100 \quad (4)$$

The concentration of hexavalent chromium in aqueous solution was analyzed using spectrometer (UV-Visible). The same analytical step method for measurement of chromium concentration has been used previously by Onchoke et al. [17].

3. RESULTS AND DISCUSSION

3.1 Fourier transformed infrared (FTIR) analysis

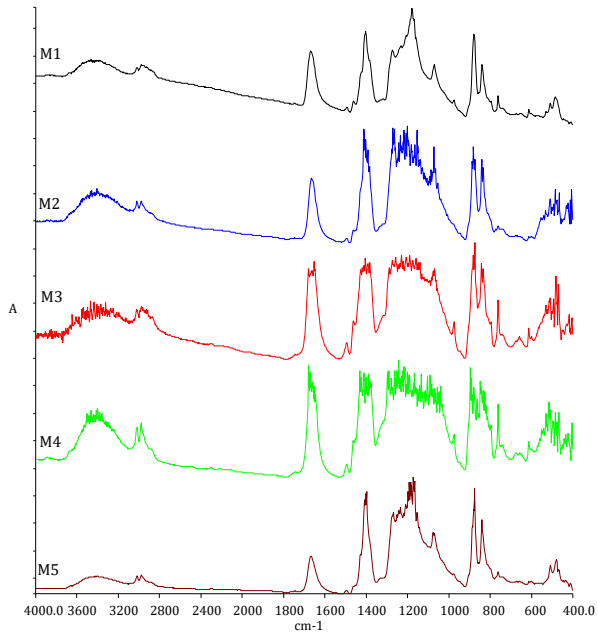

Figure 1. FTIR spectra of membrane samples

The FTIR spectra for different samples were represented in the Figure 1, The results obtained show that the membrane M1 contains functional groups of PVDF and PVP by the presence of bands situated at 3672cm^{-1} and 2898cm^{-1} assigned respectively to OH stretching, vibration band of water molecule included on the pores [18] and CH stretching band of PVDF [19]. The band situated at 1669cm^{-1} is related to C=O stretching vibration of PVP [20]. The peaks at 1495cm^{-1} and 1403 cm^{-1} represents respectively bending and waging [21, 22] vibration modes of CH_2. The band located at 1272 cm^{-1} is assigned to the OH bending vibration mode [22] At 1168cm^{-1}; it was observed strong band assigned to the CF_2 symmetric stretching and deformation modes [23]. The weak peaks located at between 509-485cm^{-1} and 444cm^{-1} was related respectively to waging and rocking modes of CF_2 [24]. The

comparison between the two FTIR spectra of the M1 and M2 membranes shows the appearance new weak bands in the spectrum of M2 membrane located at 1093cm^{-1} assigned to asymmetric stretching mode of Si-O-Si and also the band located at 479.18 cm^{-1} due to the bending mode of O-Si-O [25]. The combined effect of SG and ZnO additives is clearly apparent in the spectra of samples M3, M4 and M5 situated in the range between 460-480cm^{-1} and that's because the coupling effect of bending O-Si-O and Zn-O stretching modes [25] which can be justified by interactions during the formation of hybrid PVDF / PVP / SG / ZnO membranes.

3.2 XRD study

The XRD patterns for different membrane samples were represented in the Figure 2. respectively. XRD pattern for M1 was showed in Figure 2(a). The characteristic peaks at 2θ=17°, 20° and 10° were assigned to (022), (110) and (001) crystallographic planes which are corresponding to α crystal form of the PVDF. The other peaks located at 2θ=30°, 35° and 40° was due to the creation of new bonds and that most change in the atom's position of PVDF and PVP during the formation of the membrane M1. This is proved in comparison between the XRD patterns of PVDF and M1, it was observed the disappearance of the peak located at 2θ=27° in XRD pattern of M1 [26]. Comparison between Figure 2(b) of XRD pattern for M2 with PVDF, PVP and SG materials allows us to deduce a change in the shape of the two peaks at 2θ=17°, 20° assigned respectively to (020) and (110) symmetrical planes. On the other hand, the XRD pattern of M2 showed the appearance of new peaks located at 2θ=30°, 35° and 40°. This is due to the effect of the SG on the position of some atoms in the crystal lattice [27, 28].

The recognition of the symmetry planes of the M3 membrane is based on the information collected from the literature of XRD diagram of ZnO with diffraction pattern peaks situated at 2θ=34°, 38° and 36.22° attributed respectively to crystallographic planes (100), (002) and (101) [29-33]. The α crystal phase of PVDF was identified in the XRD pattern of M3 by the presence of symmetry planes (001), (020) and (110). The effect of adding ZnO nanoparticles was shown by comparison between the XRD pattern of M3 membrane with ZnO/SiO_2 XRD pattern [29] by crystallographic planes (002), (101), (102), (120) and (103). Comparative study between Figure 2(c), Figure 2(d) and Figure 2(e) represented respectively XRD patterns M3, M4 and M5 samples show that there is difference on the shape of peaks at 12°, 42° and 18°.

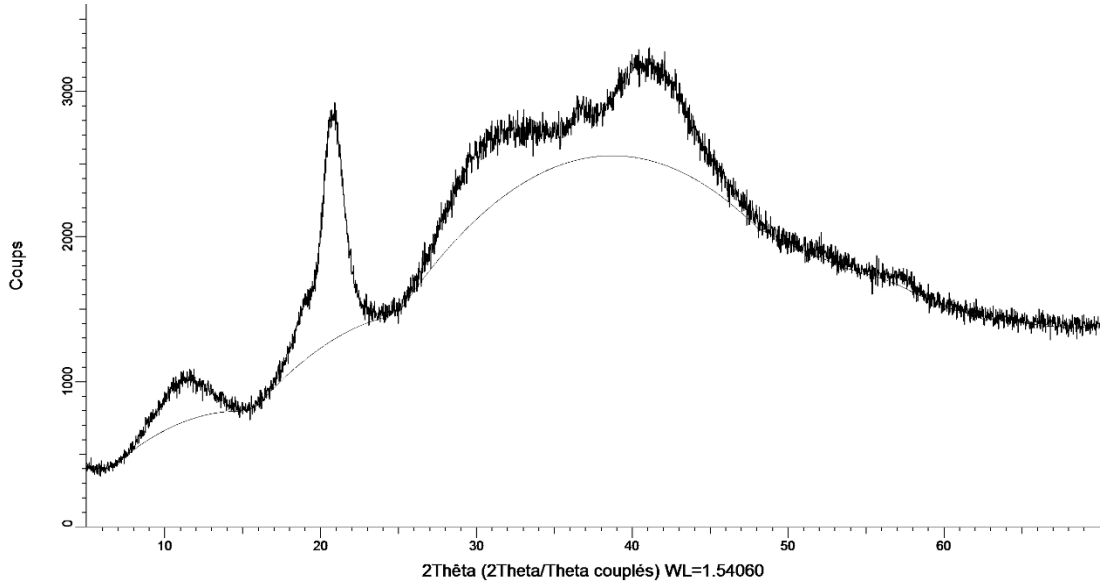

a

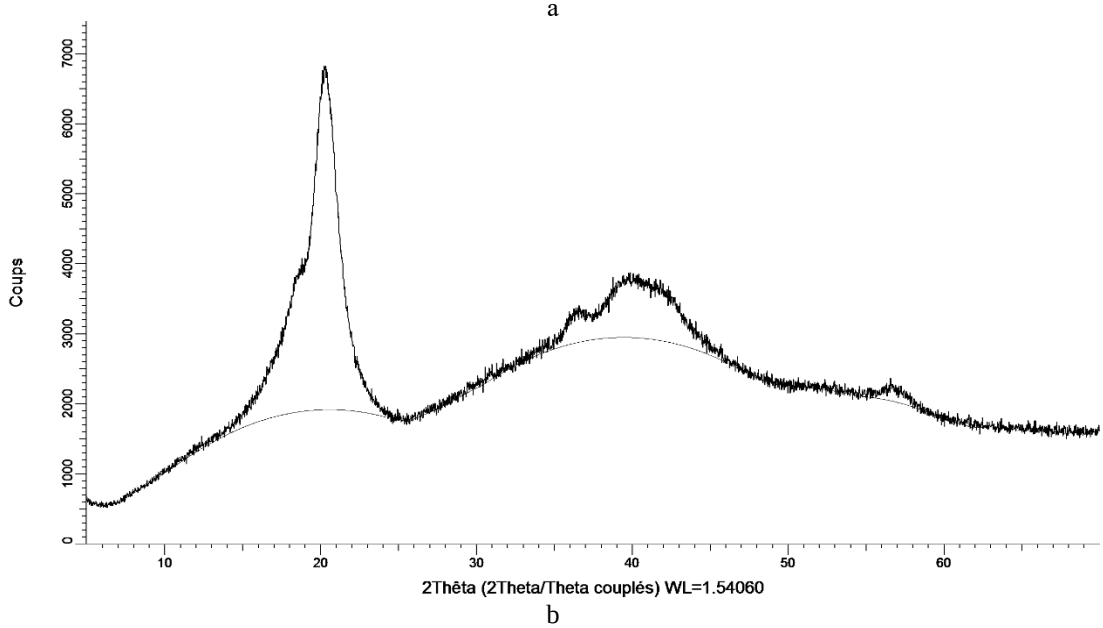

b

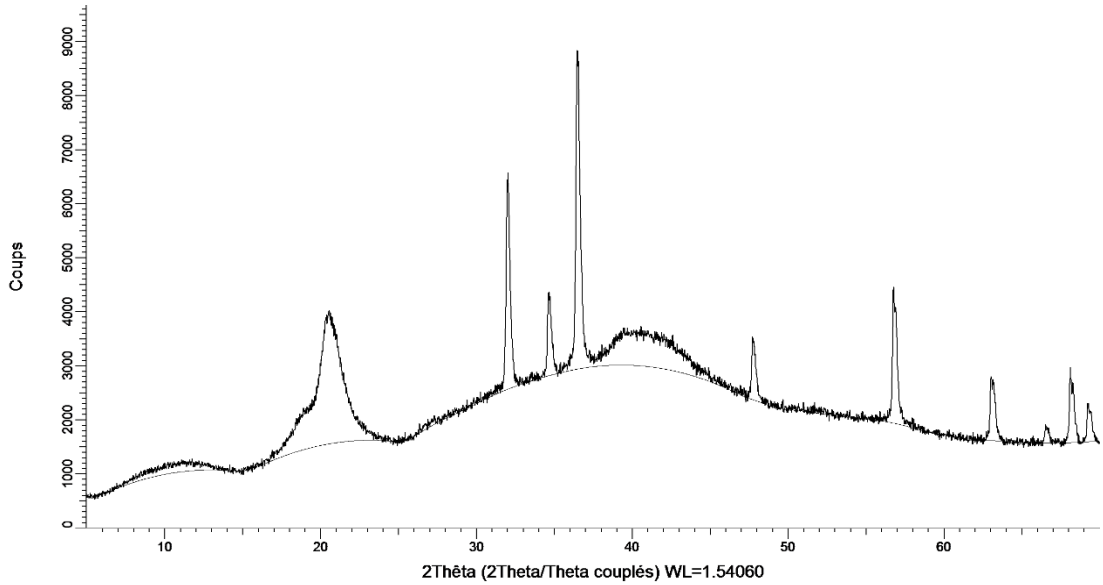

c

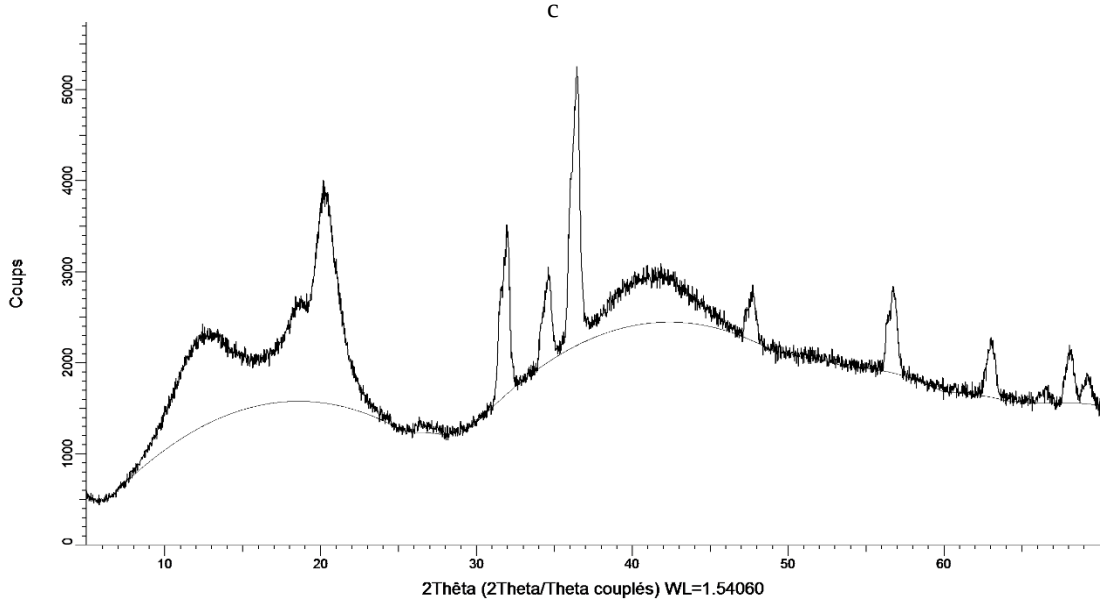

d

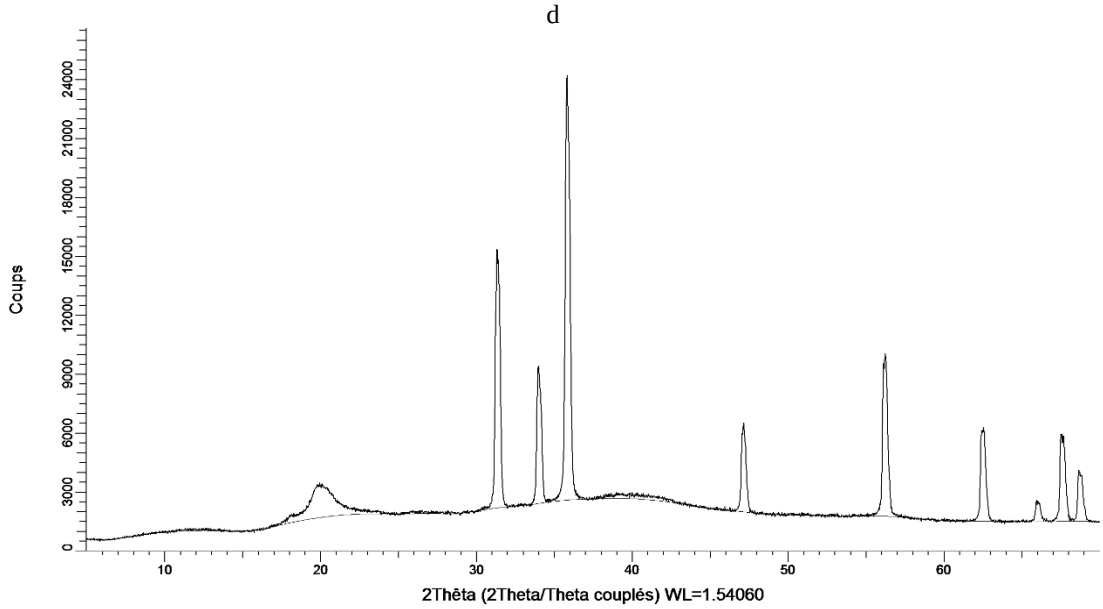

e

Figure 2. XRD patterns of membrane samples a:M1, b:M2 c:M3, d:M4, e:M5

We deduced that the increase of the ratio ZnO(%wt)/SG(%wt) in polymeric structure is accompanied with difference in the shape of the peaks and affect the arrangement of atoms in certain region. In the XRD pattern of

the M5 membrane, we recover the disappearance of the peak located at 14° (001) which corresponds to the structural atomic position of the PVDF (α phase) and a large difference in the intensities of the peaks at 20° (002) for the two samples M5 and M4, this proves the influence of ratio ZnO(%wt)/SG(%wt) on the positions of the atoms in the crystallographic planes of PVDF leading to a structural modification. This is also proved by the differences between the peaks located at 42° for the two M4 and M5 membranes.

3.3 Optical microscope analysis

The results obtained by optical microscopy shows the evolution of pore formation for the different membranes It was found that an increase in the density of the pores formed with the increase in the composition of the additives in casting solutions for each membrane. These remark est clearly apparent in Figure 3 for membrane M5 compared to the other pictures of membrane samples.

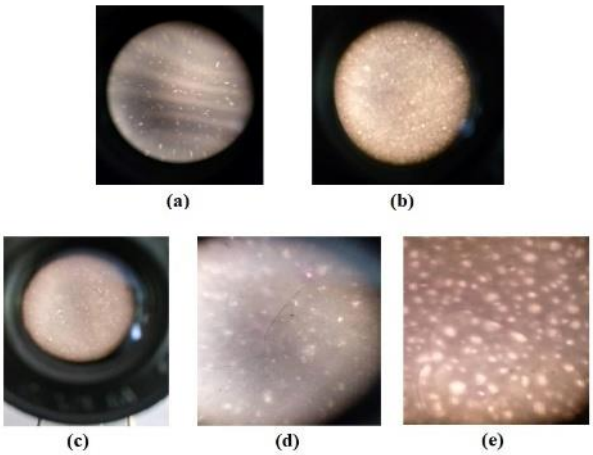

Figure 3. Pictures of the surfaces for membranes (a):M1, (b):M2, (c):M3, (d):M4, (e):M5

However, this method is considered a simple test of observation by optical microscopy which will need to be followed by other more methods.

3.4 Porosity, mean pore size and water permeability of synthesized membranes

The results presented in Table 4 and Figure 4 shows decrease of the contact angle values and increase on the values of porosity, mean pore size and pure water permeability for respectively membranes M1, M2, M3, M4 and M5.These results proves the contribution of inorganic additives (SG and ZnO) on the modification of the parameters by the increase in pure water permeability from 520 L/m^{2}hbar for M1 membrane to 679 L/m^{2}hbar for M4 membrane and 682 L/m^{2}hbar for M5 membrane. These are justified by the combined effect of SG and ZnO by creating hydrogen bonds with the water molecules, but also mobility of the PVDF polymer chains and consequently the possibility of creating new vacuum spaces and consequently increase the passage of water molecules inside the membrane matrix. Which represent a real advantage for preparation of membranes more permeable to water These results are in accordance with the data collected from the literature [31, 34]. It was found that by the increase of the weight ratio additives (ZnO/SG) from 0 to 3; the mean pores size increase from 6.55% and 17.86% for respectively membranes M1 to M5. This highlights the important contribution of ZnO nanoparticles in the modification of the membranes pores sizes.

Table 4. Porosity, pore size and water permeability measurements

Membranes	ε (%)	r_m (nm)	L_p (L/m^{2}hbar)
M1	78.88	63.44	520
M2	82.31	67.31	614
M3	83.36	71.22	644
M4	83.99	74.55	679
M5	84.05	74.77	682

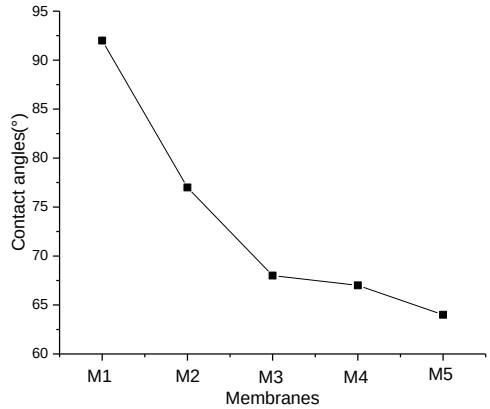

Figure 4. Contact angle measurement of membranes at 25°C

3.5 Rejection ratio of Cr (VI) by synthesized membranes

The experimental tests were carried on the dead-end pilot unit under fixed conditions (pH=6.5, T=27°C, $C_{Feed}^{Cr(VI)}$=100ppm, TMP=1.5bar). As it was shown in Figure 5, a higher rejection rate of Cr (VI) by mixed matrix membranes M2, M3, M4 and M5 in the range between 62% to 85%, these results show the combined effect SG and ZnO used as additives in the removal of hexavalent chromium from aqueous solution, these adsorbents has a very good adsorption properties, especially ZnO nanoparticles tested previously in the removal of Cu(II) ions [34]. The result of the rejection rate of Cr(VI) ions reaches 85% for a maximum weight ratio ZnO(0.75%)/SG(0.25%).

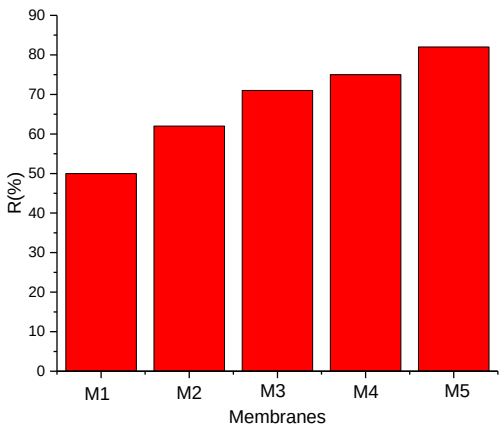

Figure 5. Cr(VI) rejection by membranes at pH=6.5 ,T=27°C, $C_{feed}^{Cr(VI)} = 100$ppm,TMP=1.5bar

4. CONCLUSION

Poly(vinylidene fluoride)(PVDF) matrix hybrid membranes mixed with poly(N-vinylpyrrolidone) (PVP), silica gel (SG) and zinc oxide (ZnO) were prepared by a phase inversion method. The pure water permeability of the matrix hybrid membranes was improved by adding silica gel and ZnO. When the content of the ratio ZnO(%wt)/SG(%wt) was 3, the pure water permeability of the hybrid matrix membranes achieved 682 L/m^2hbar and increased 31.16% compared with PVDF/PVP membrane, and the rejection ratio of Cr(VI) ions achieve 85%. In comparison with the PVDF/PVP membrane, the porosity and the mean pore size of the hybrid membranes were increased by 6.55% and 17.86%.

The hydrophilic character of matrix hybrid membranes increases with increasing the ratio ZnO(%wt)/SG(%wt). The presence of ZnO and SG in the matrix hybrid membranes was checked by the FTIR. The XRD analysis shows the different modification on atomic positions by adding ZnO and SG in polymeric structures.

REFERENCES

[1] Owlad, M., Aroua, M.K., Daud, W.A.W., Baroutian, S. (2009). Removal of hexavalent chromium-contaminated water and wastewater: A review. Water Air Soil Pollution, 200: 59-77. https://doi.org/10.1007/s11270-008-9893-7

[2] Rager, J.E., Suh, M., Chappell, G.A., Thompson, C.M., Proctor, D.M. (2019). Review of transcriptomic responses to hexavalent chromium exposure in lung cells supports a role of epigenetic mediators in carcinogenesis. Toxicology Letters, 305: 40-50. https://doi.org/10.1016/j.toxlet.2019.01.011

[3] Parlayici, S., Eskizeybek, V., Avcı, A., Pehlivan, E. (2015). Removal of chromium (VI) using activated carbon-supported-functionalized carbon nanotubes. Journal of Nanostructure in Chemistry, 5(3): 255-263. https://doi.org/10.1007/s40097-015-0156-z

[4] Peng, H., Leng, Y., Cheng, Q., Shang, Q., Shu, J., Guo, J. (2019). Efficient removal of hexavalent chromium from waste water with electro reduction. Processes, 7(1): 41. https://doi.org/10.3390/pr7010041

[5] Gurbuz, F. (2009). Removal of toxic hexavalent chromium ions from aqueous solution by a natural biomaterial: Batch and column adsorption. Adsorption Science & Technology, 27(8): 745-759. https://doi.org/10.1260/0263-6174.27.8.745

[6] Nqombolo, A., Mpupa, A., Moutloali, R.M., Nomngongo, P.N. (2018). Wastewater treatment using membrane technology. Wastewater and Water Quality, 29-40. https://doi.org/10.5772/intechopen.76624

[7] Liu, F., Hashim, N.A., Liu, Y., Abed M.R.M., Li, K. (2011). Progress in the production and modification of PVDF membranes. Journal of Membrane Science, 375(1-2): 1-27. https://doi.org/10.1016/j.memsci.2011.03.014

[8] Wang, X., Zhou, K., Ma, Z., Lu, X., Wang, L., Wang, Z., Gao, X. (2017). Preparation and characterization of novel polyvinylidenefluoride/2-aminobenzothiazole modified ultrafiltration membrane for the removal of Cr(VI) in wastewater. Polymers, 10(1): 19. https://doi.org/10.3390/polym10010019

[9] Wahab, M.Y., Muchtar, S., Jeon, S., Fang, L.F., Rajabzadeh, S., Takagi, R., Arahman, N., Mulyati, S.R., Medyan, M. (2019). Synergistic effects of organic and inorganic additives in preparation of composite poly(vinylidene fluoride) antifouling ultrafiltration membranes. Journal of Applied Polymer Science, 136(27): 1-10. https://doi.org/10.1002/app.47737

[10] Abdel-Mottaleb, M.M., Khalil, A., Osman, T.A., Khattab, A. (2019). Removal of hexavalent chromium by electrospun PAN/GO decorated ZnO. Journal of Mechanical Behavior Biomedical Materials, 98: 205-212. https://doi.org/10.1016/j.jmbbm.2019.06.025

[11] Gang, D., Banerji, S.K., Clevenger, T.E. (2000). Chromium (VI) removal by modified PVP-coated silica gel. practice periodical of hazardous. Toxic and Radioactive Waste Management, 4: 105-110. https://doi.org/10.1061/(asce)1090-025x(2000)4:3(105)

[12] Karthik, R., Meenakshi, S. (2014). Removal of hexavalent chromium ions using polyaniline/silica gel composite. Journal of Water Process Engineering, 1: 37-45. https://doi.org/10.1016/j.jwpe.2014.03.001

[13] Bai, H., Wang, X., Zhou, Y., Zhang, L. (2012). Preparation and characterization of poly(vinylidene fluoride) composite membranes blended with nano-crystalline cellulose. Progress in Natural Science, 22(3): 250-257. https://doi.org/10.1016/j.pnsc.2012.04.011

[14] Hu, Y.C., Hsu, W.L., Wang, Y.T., Ho, C.T., Chang, P.Z. (2014). Enhance the pyroelectricity of polyvinylidene Fluoride by Graphene-Oxide Doping. Sensors, 14(4): 6877-6890. https://doi.org/10.3390/s140406877

[15] Wu, G., Gan, S., Cui, L., Xu, Y. (2008). Preparation and characterization of PES/TiO_2 composite membranes. Applied Surface Science, 254(21): 7080-7086. https://doi.org/10.1016/j.apsusc.2008.05.221

[16] Hong, J., He, Y. (2012). Effects of nano sized zinc oxide on the performance of PVDF microfiltration membranes. Desalination, 302: 71-79. https://doi.org/10.1016/j.desal.2012.07.001

[17] Onchoke, K.K., Sasu, S.A. (2016). Determination of hexavalent chromium (Cr(VI)) concentrations via ion chromatography and UV-Vis spectrophotometry in samples collected from Nacogdoches waste water treatment plant, East Texas (USA). Advances in Environmental Chemistry, 1-10. https://doi.org/10.1155/2016/3468635

[18] Ngang, H.P., Ahmad, A.L., Low, S.C., Ooi, B.S. (2017). Preparation of PVDF/SiO_2 composite membrane for salty oil emulsion separation: Physicochemical properties changes and its impact on fouling propensity. IOP Conference Series Materials Science and Engineering, 206(1): 012083. https://doi.org/10.1155/2016/3468635

[19] Guo, Z., Xu, X., Xiang, Y., Lu, S., Jiang, S.P. (2015). New anhydrous proton exchange membranes for high-temperature fuel cells based on PVDF–PVP blended polymers. Journal of Materials Chemistry A, 3(1): 148-155. https://doi.org/10.1039/C4TA04952G

[20] Liao, C., Zhao, J., Yu, P., Tong, H., Luo, Y. (2012). Synthesis and characterization of low content of different SiO_2 materials composite poly(vinylidene fluoride) ultrafiltration membranes. Desalination, 285: 117-122. https://doi.org/10.1016/j.desal.2011.09.042

[21] Asmatulu, R., Jabbarnia, A. (2015). Synthesis and characterization of PVDF/PVP-based electrospun

membranes as separators for super capacitor applications. Journal of Material Science and Technology Research, 2(2): 43-51. https://doi.org/10.15377/2410-4701.2015.02.02.3
[22] Wu, T., Zhou, B., Zhu, T., Shi, J., Xu, Z., Hu, C., Wang, J. (2015). Facile and low-cost approach towards a PVDF ultrafiltration membrane with enhanced hydrophilicity and antifouling performance via graphene oxide/water-bath coagulation. RSC Advance, 5(11): 7880-7889. https://doi.org/10.1039/C4RA13476A
[23] Jaleh, B., Gavary, N., Fakhri, P., Muensit, N., Taheri, S. (2015). Characteristics of PVDF membranes irradiated by electronbeam. Membranes, 5(1): 1-10. https://doi.org/10.3390/membranes5010001
[24] Boccaccio, T., Bottino, A., Capannelli, G., Piaggio, P. (2015). Characterization of PVDF membranes by vibrational spectroscopy. Journal of Membrane Science, 210(2): 315-329. https://doi.org/10.1016/S0376-7388(02)00407-6
[25] Sivaiah, K., Kumar, K., Naveen, N., Naresh, V. (2011). Structural and optical properties of Li+: PVP & Ag+: PVP polymer films. Materials Sciences and Applications, 2(11): 1688-1696. https://doi.org/10.4236/msa.2011.211225
[26] Satapathy, S., Pawar, S., Gupta, P.K., Varma, K.B.R. (2011). Effect of annealing on the phase transition in poly (vinylidene fluoride) films prepared using polar solvent. Bulletin of Materials Science, 34(4): 727-733. https://doi.org/10.1007/s12034-011-0187-0
[27] Nandanwar, R., Singh, P.Z., Haque, F. (2015). Synthesis and characterization of SiO_2 nanoparticles by sol-gel process and its degradation of methylene blue. American Chemical Science Journal, 5(1): 1-10. https://doi.org/10.9734/ACSJ/2015/10875
[28] Setia, U., Panca, Y.R., Sangwichien, C. (2018). Silica gel derived from palm oil mill fly ash. Songklanakarin Journal of Science and Technology, 40(1): 121-126. https://doi.org/10.14456/sjst-psu.2018.27
[29] Chen, Y., Ding, H., Sun, S. (2017). Preparation and characterization of ZnO nanoparticles supported on amorphous SiO_2. Nanomaterials, 7(8): 217. https://doi.org/10.3390/nano7080217
[30] Taha, A.K.T., Amir, M., Demir Korkmaz, A., Al-Messiere, M.A., Baykal, A., Karakuş, S., Kilislioglu, A. (2018). Development of novel Nano-ZnO enhanced polymeric membranes for water. Purification. Journal of Inorganic and Organometallic Polymers and Materials, 29(3): 979-988. https://doi.org/10.1007/s10904-018-0988-3
[31] Zhang, X., Wang, Y., Liu, Y., Xu, J., Han, Y., Xu, X. (2014). Preparation, performances of PVDF/ZnO hybrid membranes and their applications in the removal of copper ions. Applied Surface Science, 316(1): 333-340. https://doi.org/10.1016/j.apsusc.2014.08.004
[32] Bhuiyan, M.R.A., Rahman, M.K. (2014). Synthesis and characterization of Ni doped ZnO nanoparticles. International Journal of Engineering and Manufacturing, 4(1): 10-17. https://doi.org/10.5815/ijem.2014.01.02
[33] Hong, J., He, Y. (2012). Effects of Nano sized zinc oxide on the performance of PVDF microfiltration membranes. Desalination, 302: 71-79. https://doi.org/10.1016/j.desal.2012.07.001
[34] Alaei Shahmirzadi, M.A., Kargari, A. (2018). Nanocomposite membranes, emerging technologies for sustainable. Desalination Handbook, 285-330. https://doi.org/10.1016/B978-0-12-815818-0.00009-6

NOMENCLATURE

A_m	Membrane filtration area (m^2)
V	Volume of the permeate (L)
t	time (h)
TMP	transmembrane pressure (bar)
Q_w	Pure water flow (m^3/s)
ΔP	Operating pressure test (Pa)
R(%)	Rejection ratio of Cr (VI) by membranes
$C_{permeate}^{Cr\ (VI)}$	Concentration of Cr (VI) in feed (ppm)
$C_{Feed}^{Cr\ (VI)}$	Concentrationof Cr (VI) in permeate (ppm)
L_p	Pure water permeability (L/m^2hbar)
r_m	Average pore size (nm)

Greek symbols

ε	Porosity of the membrane (%)
ρ_p	The density of the polymer (g/cm^3)
ρ_{water}	The density of water (g/cm^3)
ξ	Membrane thickness (nm)
η	Water viscosity (8.9×10^{-4} Pa.s)

Subscripts

SG	Silica gel
PVP	Poly(N-vinylpyrrolidone)
PVDF	Polyvinylpyrrolidone
PAN	Polyacrylonitrile
PANI	polyaniline
FTIR	Fourier transform infrared spectroscopy
XRD	X-ray diffraction
GO	Graphene oxide